ISSN 1392 - 1207. MECHANIKA. 2012 Volume 18(3): 285-291

Fatigue strength investigation of four type cast irons specimens

M.K. Leonavičius*, E. Stupak, A. Krenevičius***, A. Norkus******
**Vilnius Gediminas technical university, Saulėtekio al. 11, 10223, Vilnius-40, Lithuania,
E-mail: mindaugas.leonavicius@vgtu.lt*
***Vilnius Gediminas technical university, Saulėtekio al. 11, 10223, Vilnius-40, Lithuania,
E-mail: Eugenius.Stupak@vgtu.lt*
****Vilnius Gediminas technical university, Saulėtekio al. 11, 10223, Vilnius-40, Lithuania, E-mail: kron@vgtu.lt*
*****Vilnius Gediminas technical university, Saulėtekio al. 11, 10223, Vilnius-40, Lithuania,
E-mail: arnoldas.norkus@vgtu.lt*

crossref http://dx.doi.org/10.5755/j01.mech.18.3.1882

1. Introduction

Castings after some mechanical treatment and taking into account part purpose in the structure, could be used according required function in the equipment. But there exist some casts, when during the production stage should be used modification, specific cooling or thermal treatment. After selection of chemical composition and satisfying stages of production process the required microstructure, static mechanical properties and resistance for cyclic and dynamic loading [1-9] are obtained.

For quality of cast iron casting are important quantity of graphite, size and shape of inserts, and its interaction. Small deviation from the rules of production process, increase or decrease of alloyed element quantity change significantly casting and mechanical properties of cast irons. In manuals presented mechanical properties indices and endurance limit values are not enough parameters for responsible parts, so additional qualifying analytical experimental tests should be done. Tests used for comparison are done also, when structural element's material should be selected from few variants. Determination of material's resistance to cyclic loading using fracture mechanics [1-9] rules is long lasting and expensive.

This paper presents the four type cast irons comparative investigation results, when static mechanical properties and durability properties, using standard experimental methodologies are determined. In all investigated cast irons types the chemical composition or production process are changed in order to decrease production price or have better properties. After analysis of the obtained results it is possible to make decision about of cast iron suitability for production of mining mineral equipment parts, or possibility of thermal treatment. Taking into account chemical composition, microstructure and mechanical properties one could make decision about cast iron suitability for the production of austempered ductile cast iron (ADI).

2. Problem formulation

Properties of large size cast are dependent of structure metallic base and rate of graphite spheroidisation. Chemical composition is one of the major factor influencing cast iron mechanical properties. Chemical composition for investigated cast irons is presented in Table. In the high strength cast iron, quantity of carbon constitutes 3.1-3.7%. For the high clearance parts, the quantity of carbon may be reduced, so as to increase casting features.

Table

Chemical composition, Wt %

Cast iron	C	Si	Mn	Ni	Mo	Cu	Cr
CI-1	3.6	1.75	0.87	0.50	0.52	0.52	0.062
CI-2	3.6	2.6	0.40	0.10			0.10
CI-3	3.7	2.9	0.08	0.14	0.02	0.24	0.036
CI-4	3.1	3.8	0.05			0.04	

The quantity of alloying elements contributes to the regulation of metallic [10-12] basis and process of graphitization. In order a pearlite structure comprises in such castings, cast iron is alloyed by nickel or cupper. The quantity of vanadium and chromium is also limited (not more than 0.1%), as they stimulate formation of carbides. By decreasing the rate of cooling a great quantity of ferrite might form. Ferrite reduces mechanical properties, while carbide-phosphide derivatives form themselves on the surfaces of euthectic crystallites. Silicon alloyed cast iron CI-4 price is lower, but mechanical properties are not high. It could be used at specific environment conditions, if mechanical properties are obtained. Using such cast iron with higher silicon quantity thin walled parts can be made also. In order to satisfy graphite formation process casting should satisfy product quality requirements [1-3, 7, 8].

Micrographs of cast irons microstructure are presented in Fig. 1. The obtained required structure is presented in Fig. 1, a, c, e, g, while inhomogeneities are observed in Fig. 1, b, d, f, h. Cast iron have pearlite matrix with spherical graphite inserts surrounded by ferrite layer. This typical graphite view is usually named as "bull's eye". Smaller ferrite shell is effective because it improves mechanical properties of cast iron: brittle and soft graphite surrounded by ferrite layer stop short and long crack propagation. Graphite inserts and their shells shape and distribution are not uniform, there are insert with poor regular spheroid shape. Changing of the structure in the part volume has significant influence on properties of high strength cast iron, which microstructure is rather complicated. It is complicated to satisfy the same cooling conditions and speed for big dimensions castings, specimens cute of them are used in present investigation.

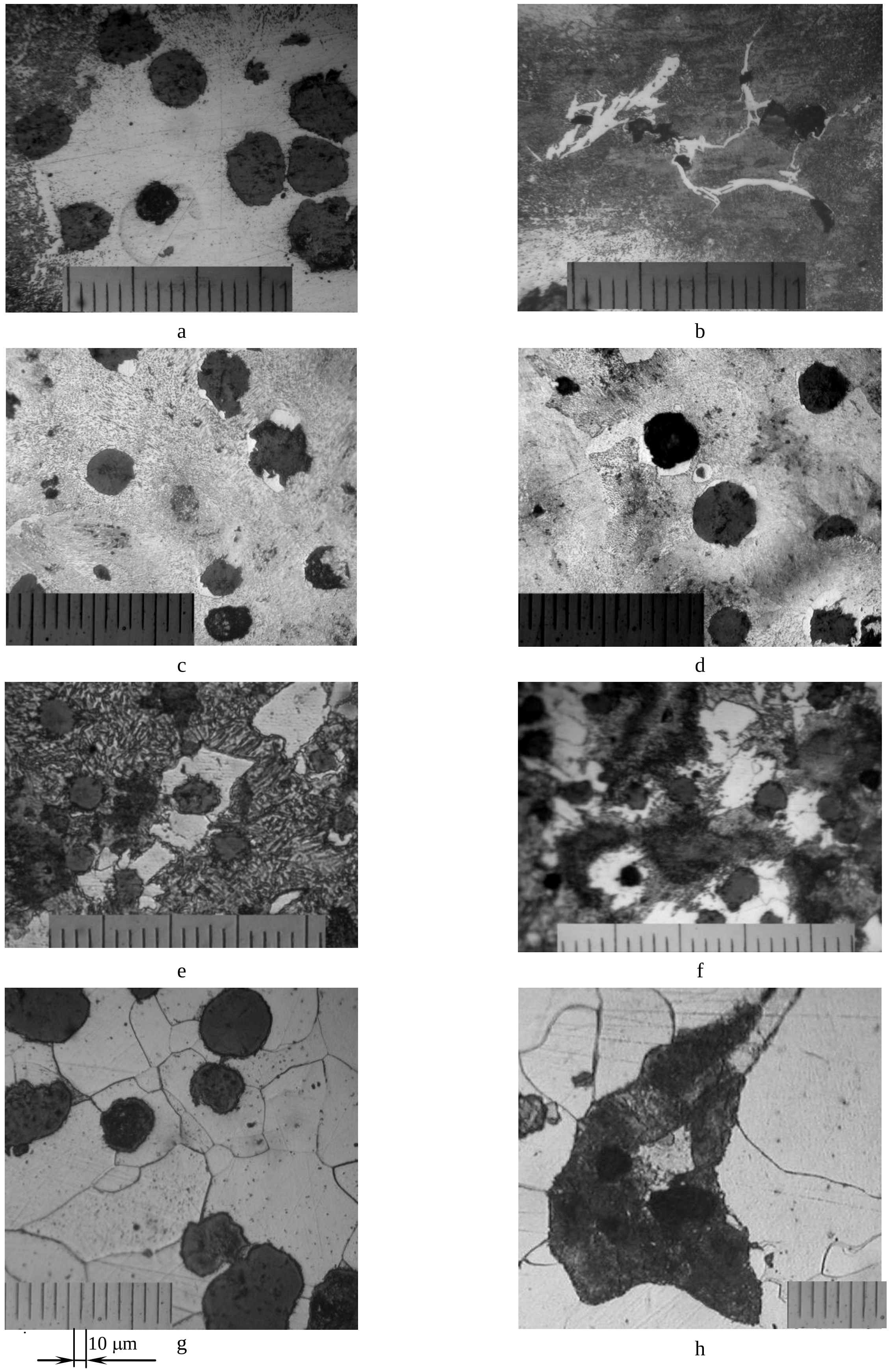

Fig. 1 Micrographs of microstructure for CI-1 (a, b); CI-2 (c, d); CI-3 (e, f); CI-4 (g, h)

Cast iron’s CI-3 microstructure (Fig. 1, e) consist of spheroid graphite surrounded by ferrite and metal base of ferrite and pearlite platelets. Some observed structure anomalies and/or defects allow considering the static and cyclic strength in different specimens. Microstructures of the investigated cast iron with higher silicon CI-4 are presented in Fig. 1, g, h. Microstructure analysis shows that the structure consists of ferrite (grain dimension reaches 0.25 mm) and spherical graphite (grain similar to globule is till 0.1 mm). During the cast iron mould occur the defects so called “black marks or spots”. In common case this is the accumulations of magnium sulfides and graphites. The study of chemical composition shows higher quantity of carbon and sulphur in these places. It is possible to decrease quantity of “black spots” using higher temperature of casting, applied flux (such as natrium carbonate, etc.) for melted metal, but it is rather complicated have not it at all [7]. The microstructure is presented in Fig. 1, g. It shows the microstructure of etched cast iron CI-4, where are clearly observed graphite grains of various size and shape and nodules of spheroidal graphite. The microstructure in Fig. 1, h shows clearly existence of heterogeneous anomalies.

For static mechanical properties determination there were used the cylindrical specimens: diameter d = 8-14 mm; original gauge length – 25-50 mm. The obtained mechanical properties are as follow: for cast iron CI-1 yield strength $\sigma_{0.2}$ = 329-360 MPa; tensile strength σ_u = 472-476 MPa; modulus of elasti-city E = 153-166 GPa; percentage elongation A_t = 11.2-12.2%; Brinell hardness HB = 180-190. For CI-2: ($\sigma_{0.2}$ = 360-389 MPa; σ_u = 574-578 MPa; E = 146-148 GPa; A_t = 2.5-2.8%; HB = 220-225). For CI-3: ($\sigma_{0.2}$ = 387-414 MPa; σ_u = 620-692 MPa; E = 150-162 GPa; A_t = 8.2-12.4%; HB = 203-224). For CI-4: ($\sigma_{0.2}$ = 322-329 MPa; σ_u = 403-449 MPa; E = 160-164 GPa; A_t = 5.4-17.3%; HB = 156-61).

The analysis showed that the cast irons are sufficiently ductile – relative elongation reach 17.3% the obtained chemical composition, microstructure and static mechanical properties of cast irons justify about its suitability for structural elements production or thermal treatment.

3. Durability

Specimens with continuous radius have been prepared according standard requirements [13] and were used for determining endurance limit, while notched tensile specimens were used for the investigation of fracture history. In Fig. 2 the specimens used for fatigue investigation are shown.

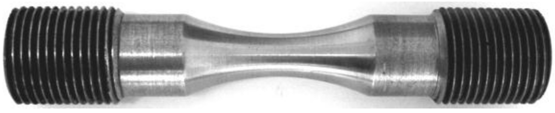

a

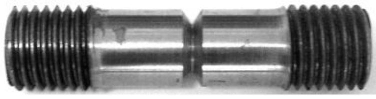

b

Fig. 2 Specimens: with continuous radius (a) and notched tensile (b)

It were the specimens with continuous radius d_{min} = 10.7 mm and cylindrical specimens d = 17.8 mm with circular notch d_{min} = 10.7 mm (notch radius R = 0.25 mm).

Some specimens with continuous radius have been tested in the range till $N = 10\times10^6$-20×10^6 fatigue cycles, with stress asymmetry ratio $r \approx 0$ and endurance limits have been obtained as follows: for CI-1 – σ_0 = 180 MPa; for CI-2 – σ_0 = 170 MPa; for CI-3 – σ_0 = 220 MPa; for CI-4 – σ_0 = 160 MPa.

Typical breaks of the specimens with circular notch (Fig. 2, b) are presented in Fig. 3. Maximum cyclic stress level has been changed and crack initiation has been controlled using undamaging techniques till fracture of specimens. All specimens have been broken at the weakest place. The break of one specimen (of cast iron CI-4) occurred not in the weakest place, but at the so called “black spots” type defect as presented in Fig. 3, d at the $N = 10^5$ cycles. White different size grains are observed in all breaks. In the specimen break on Fig. 3, f are obtained rather large shrinkage areas and “black spots” in the vicinity of them. “Surface defects have been observed before the test and had the influence on fatigue crack initiation and propagation during all cyclic load history.

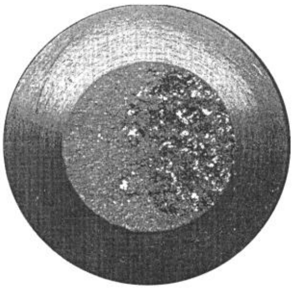

a

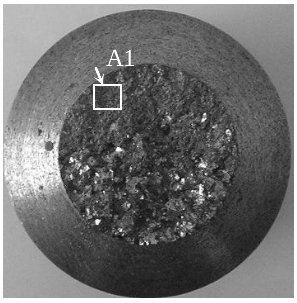

b

c

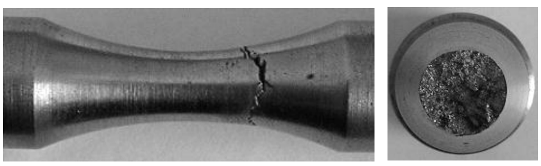

d

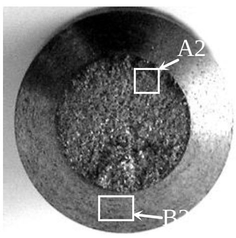

e

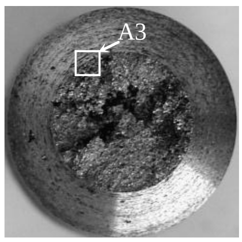

f

Fig. 3 Breaks of notched specimens: a – CI-1; b – CI-2; c – CI-3; d-f – CI-4

Advanced analyses of breaks have been performed using scanning electron microscope (SEM) and the views are presented in Fig. 4. SEM views and breaks views presented in Fig. 3 have relation with all cast irons micrographs from Fig. 1. Macropores, pores [14] and inhomogeneous formations in the bottom of the notch became origins of cracks (Figs. 3 and 4)

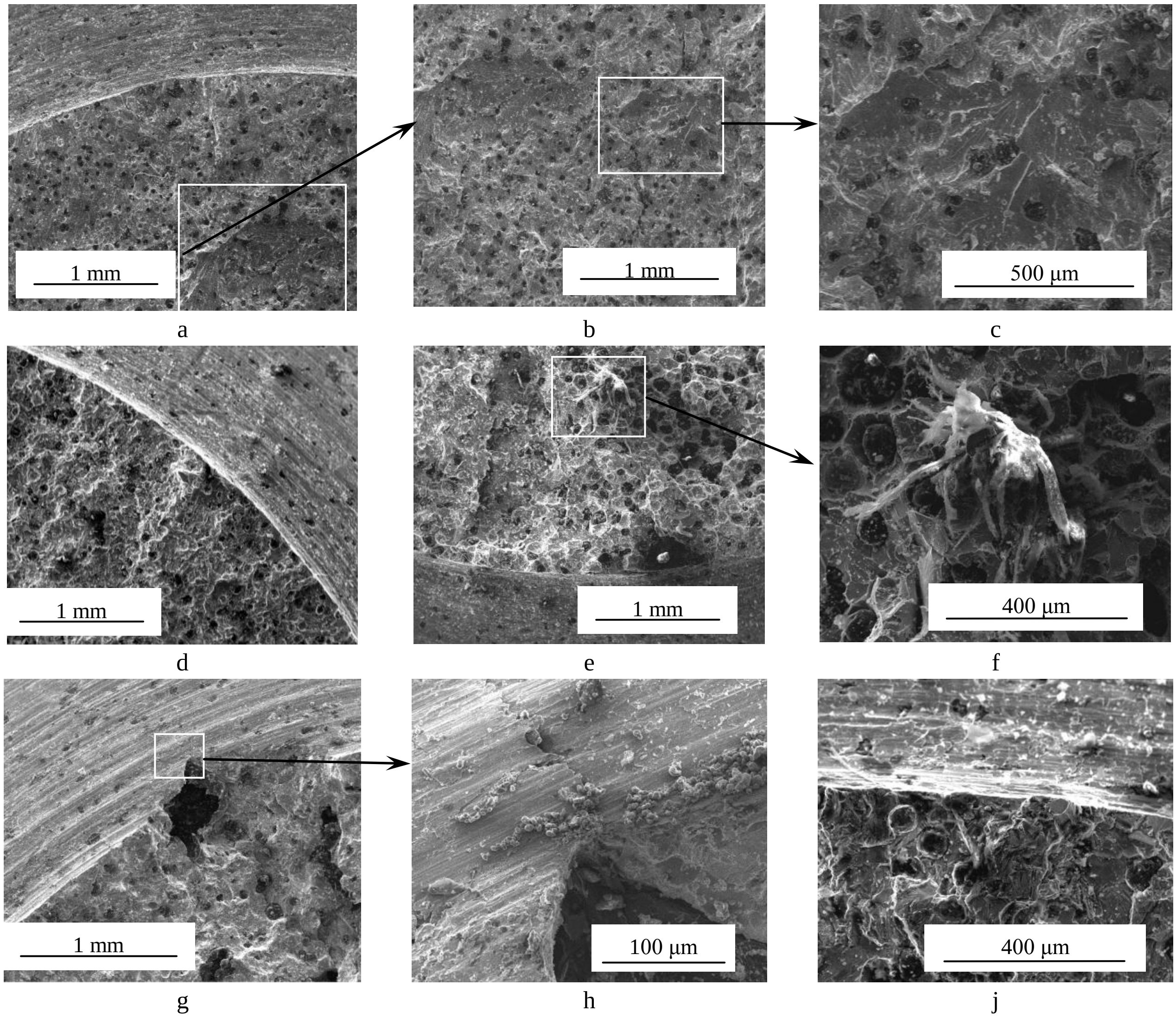

Fig. 4 Views obtained by SEM: a-c – CI-2; d-f – CI-4 (Fig. 3, e); g-j – CI-4 (Fig. 3, f)

Fatigue fracture is driven by several fracture mechanisms at once, e.g. at inter grained surfaces or through the grains. Stress state, microstructure and other factors at local place are favourable for mixed cracking type.

On the views presented in Fig. 4, a-c one should observe the fracture plane change at some small area, at its' edges is cleavage fracture mechanism, while on its bottom splitting fracture mechanism is dominating.

The view near the fatigue zone having specific features of cast iron CI-4 specimen (Fig. 3, e) is presented in Fig. 4, d, while Fig. 4, e, f presents brittle zone with clearly expressed modified crack front and changed cracking mechanism (splitting and cleavage at once). It is related with inhomogeneous microstructure of cast iron CI-4 (Fig. 1) and various grains size and shape. The view obtained by SEM and presented in Fig. 4, f express the top of the crest surrounded by crumbled and placed in the matrix nucleus respectively.

Macrovoids of cast iron CI-4 specimen with surface defects (Fig. 3, f) presented in Fig. 4, g, h became one of the crack origins. Pores and microvoids and macrovoids on this specimen have been placed on fractures' surface and decreased significantly number of cycles to full failure.

Facets observed in Fig. 4, c and Fig. 4, j have some boundaries visible on some places of break surface. They are formed under brittle inter-granular failure as well as ductile failure mechanism

Fatigue curves obtained for specimens cute from large dimensions cast plates with circular notch made of 4 types of the investigated cast irons are presented in Fig. 5. Endurance limits have been obtained in the range till $N = 15\times10^6$-30×10^6 fatigue cycles, with stress asymmetry ratio $r \approx 0$. The presented experimental durability data show significant decreasing of cycles number if some inhomogeneities or pores are observed in notched specimens. An line obtained by approximation function "1" for cast iron "CI-2" is different than for cast irons CI-1, CI-3, CI-4 and this is related with small percentage elongation A_t = 2.5-2.8 %, having influence on cracking at larger stress level.

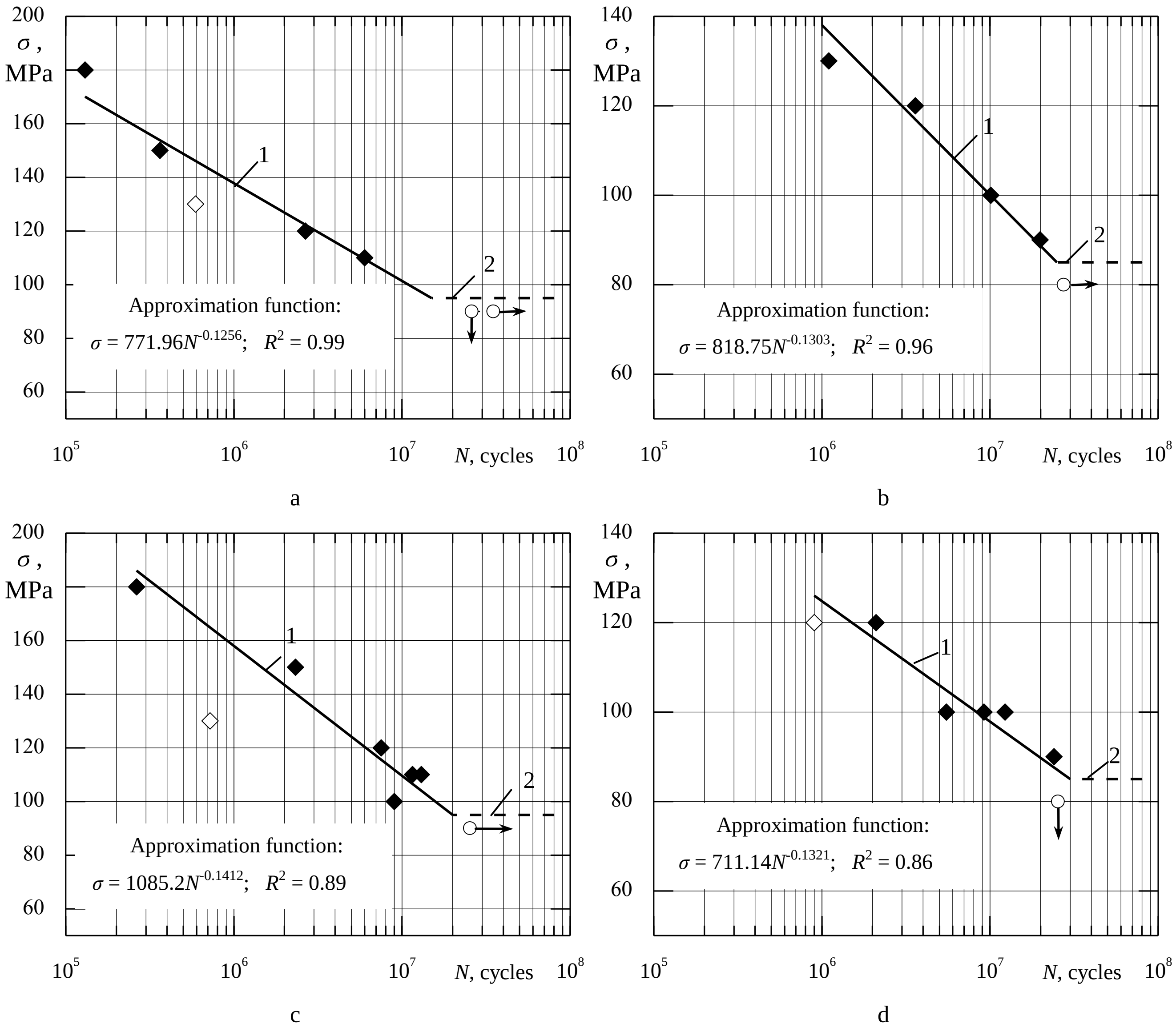

Fig. 5 Cycle strength of specimens with circular notch: CI-1 (a); CI-2 (b); CI-3 (c); CI-4 (d); where *1* – approximation function; *2* – endurance limit; ◆, ◇ – specimens with homogeneous and inhomogeneous structure or defects respectively; ○↓ – statically broken specimen; ○→ – specimen not broken

4. Analytical results

The values of stress intensity factor K_C have been determined for fatigue breaks of experimentally tested notched specimens. Fig. 6 shows a schema used for the analysis of all four types' cast iron specimens' breaks. Yarema [15] taking into account Neiber interpolation function proposed equation useful for determining stress intensity coefficient of smooth specimens with external crack with changed depth.

For the break of specimen stress intensity coefficient is calculated as

$$K_C = \frac{\sqrt{\pi R(\beta)}}{2} \sqrt[4]{1+x^2} \left[\frac{\sigma_f}{\sqrt{1+g}} + \frac{3}{4} \frac{\sigma_b}{\sqrt{1+0.5625g}} \right] \quad (1)$$

where σ_f and σ_b nominal stress caused by tension force F and bending moments respectively:

$\sigma_f = \frac{F}{\pi ab}$; $\sigma_b = \frac{4}{\pi ab}\left(\frac{M_y r}{a^2} \sin\beta + \frac{M_x r}{b^2} \cos\beta \right)$. Bending moments M_x and M_y could be expressed as follows $M_x = Fr_0 \sin\gamma$ and $M_y = Fr_0 \cos\gamma$; $R(\beta)$ is equation of die described in polar coordinates r, β, with centre coincident of ellipse centre. It could be expressed as $r = R(\beta) = ab(a^2 \cos^2\beta + b^2 \sin^2\beta)^{-0.5}$ or $r = \sqrt{R^2 - 2sR\cos\psi + s^2}$ is the distance from ellipse center point to the point on normal to the contour, where s is the distance along normal from contour, R is radius-vector, ψ is an angle between the normal in point on contour (R, β) and it's radius-vector R. Cosine of an angle is described as $\cos\psi = (1+x^2)^{-0.5}$, here $x = \frac{1}{R}\frac{\mathrm{d}R}{\mathrm{d}\beta}$;

$g = 0.199h^{-1}R(1+x^2)^{0.5}$;

$$h = \frac{R(\beta)}{\sqrt{1+x^2}} \left\{ \left[\lambda^2 \left(1+x^2\right) - \left(x + \mu \sin\delta\right) - x\mu \cos\delta \right]^{0.5} - 1 + \mu(\cos\delta + x \sin\delta) \right\}$$

where $\delta = \beta - \gamma$, $\lambda = D/2R$, $\mu = r_0 / R$, r_0, γ are coordinates in polar coordinate system of intersection point between rod axis and ellipse diaphragm plane.

During the testing of cast iron cylindrical notched specimens with an ellipse, which centre is as one of the rod axies, shape cracks (Fig. 6, b) formula of stress intensity factor is simplified. In this case: $M_x = Fr_0$, $M_y = Fr_0 \cos\gamma = 0$, because an angle $\gamma = 90°$. For point on the contour of ellipse chord lying on axis y: $\beta = 0$; radius-vector $R = b$; $h = D/2 + r_0 - b$; normal stress due to bending $\sigma_b = 4Fr_0 / (\pi a b^2)$.

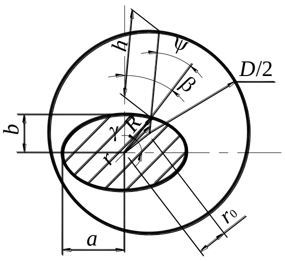

a

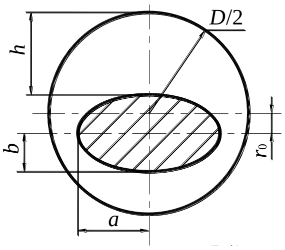

b

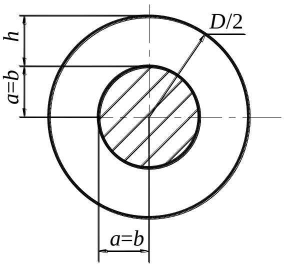

c

Fig. 6 Schema for determination of stress intensity factor, when ellipse is moved: in axes *x* and *y* direction (a), only in axis *y* direction (b); in the case of circle (c)

In this case stress intensity factor

$$K_C = \frac{\sqrt{\pi b}}{2} \left[\frac{\sigma_f}{(1+0.199\, b\, h^{-1})^{0.5}} + \frac{3}{4} \frac{\sigma_b}{(1+0.112\, b\, h^{-1})^{0.5}} \right] \quad (2)$$

For the single specimens when diaphragm is circular (Fig. 6, c) $a = b = R$ and $r_0 = 0$ and stress intensity factor

$$K_C = \frac{F}{2\sqrt{\pi R^3}} \left[1 - \frac{0.199\, R}{D/2 - 0.801\, R} \right]^{0.5} \quad (3)$$

The performed analysis of notched specimens breaks shows, that in some of them crack propagation path is not clearly observed, final fully cyclic fracture zone is not clearly shaped also. Measurements of fractured surfaces have been done using optical and mechanical measuring instruments. Breaks initial diagrams have been unified as one of the cases presented in Fig. 6. For all cases (when ellipse is moved: in axies *x* and *y* direction; or only in axis *y* direction; or in the case of circle) required parameters of *D*, *a*, *b*, *h*, r_0 have been investigated.

Values of stress intensity factors have been determined for specimens with some clearly shaped brittle zone only and are as follow: 1) for cast iron CI-1 K_c = 16-26 MPa$\sqrt{\text{m}}$; 2) for CI-2 K_c = 10-12 MPa$\sqrt{\text{m}}$; 3) for CI-3 K_c = 11-30 MPa$\sqrt{\text{m}}$; 4) for CI-4 K_c = 11-15 MPa$\sqrt{\text{m}}$.

Dispersion of the obtained results is large and it's difference with the obtained using CT specimens, where K_c = 30-70 MPa$\sqrt{\text{m}}$, is big also. Various heterogeneity zones and defects collections have an influence on crack propagation and future fracture due to cyclic loading.

The results obtained in this investigation could be applied for primary material suitability evaluation. During design of responsible structural elements some additional experiments with CT specimens or other specimens should be performed under the limited results analysis condition.

5. Conclusions

The results of the simulation may be summarised as follows:

1. The analytical and experimental analysis of four types cast irons chemical composition, microstructure, mechanical properties, cyclic fracture relations is performed in order to determine cast irons suitability for structural elements production.

2. Obtained above mentioned properties allow to decide about cast irons suitability for austempered ductile cast iron ADI production also.

3. The performed experimental cylindrical notched specimens cyclic fracture analysis and the obtained endurance limit value at stress asymmetry ratio $r \approx 0$ show the complexity of full fracture process.

4. The obtained values of stress intensity factor K_c for all types of cast irons show that investigated specimens' suitability for cyclic fracture parameters determination is rather poor.

Acknowledgement

Infrastructure of Scientific Center of Vilnius Gediminas Technical University was employed for the investigations and dr. Liudas Tumonis technical assistance with SEM.

References

1. **Schive, J.** 2009. Fatigue of Structures and Materials, Springer, 622p.
http://dx.doi.org/10.1007/978-1-4020-6808-9.
2. **Suresh, S.** 2010. Fatigue of Materials, Cambridge: Cambridge University Press, 680p.
3. **Anderson, T.L.** 2005. Fracture Mechanics. Fundamentals and Applications, Boston: CRC Press, Inc. 870p.
4. **Stupak, E.** 2010. Investigation of fracture of inhomogeneous cast iron specimens, Mechanika 1(81): 20-24.
5. **Leonavičius, M.K.; Krenevičius, A.; Bacevičius, J.** 2010. Influence of structure and mechanical properties for cyclic fracture rates of cast iron, Mechanika 2(82): 14-20.
6. **Daunys, M.; Česnavičius, R.** 2010. Investigation of low cycle asymmetric torsion, Mechanika 6(86): 5-10.
7. **Goodrich, G.M.** 1997. Cast iron microstructure anomalies and their cause, AFS Transactions, American Foundry Society, 669-680.
8. **Franceniuk, I.V.; Franceniuk, L.I.** 2004. Microstructure of Cast Iron, Steels and Non-Ferrous Alloys, Moscow, 192 p. (in Russian).
9. **Žiliukas, A.; Surantas, A.; Žiogas, G.** 2010. Strength and fracture criteria application in stress concentrator areas, Mechanika 3(83): 17-20.
10. **Jankovski, V.; Atkočiūnas, J.** 2011. Biparametric shakedown design of steel frame structures, Mechanika 17(1): 5-12.
http://dx.doi.org/10.5755/j01.mech.17.1.196.
11. **Balevičius, R.** 2010. On the prediction of non-linear creep strains, Journal of Civil Engineering and Management 16(3): 382-386.
http://dx.doi.org/10.3846/jcem.2010.43.
12. **Kala, Z.; Puklicky, L.; Omishore, A.; Karmazinova, M.; Melcher J.** 2010. Stability problems of steel-concrete members composed of high-strength materials, Journal of Civil Engineering and Management 16(3): 352-362.
http://dx.doi.org/10.3846/jcem.2010.40.
13. ASTM E 111-88. Standard Test Method for Young's Modulus, Tangent Modulus, and Chord Modulus.
14. **Amšiejus, J.; Kačianauskas, R.; Norkus, A.; Tumonis,L.** 2010. Investigation of the sand porosity via oedometric testing, The Baltic Journal of Road and Bridge Engineering 5(3): 139-147.
http://dx.doi.org/10.3846/bjrbe.2010.20.
15. **Jarema, S.J.** 1970. Stress intensity factors for cylindrical specimens with external different depth crack, Physical-Chemical Mechanics of Materials 1: 87-89 (in Russian).

M.K. Leonavičius, E. Stupak, A. Krenevičius, A. Norkus

KETURIŲ KETAUS RŪŠIŲ BANDINIŲ CIKLINIO STIPRUMO TYRIMAS

R e z i u m ė

Pateikti duomenys apie keturių ketaus rūšių cheminę sudėtį, struktūrą, statinių mechaninių savybių rodiklius, patvarumą ir ciklinio irimo tąsumą. Tiriant cilindrinius bandinius, kurių skersmuo 8-14 mm, nustatyta, kad stiprumo riba σ_u = 403-692 MPa. Cikliškai apkraunant cilindrinius bandinius su žiedine išpjova nustatyta patvarumo riba σ_0 = 85-96 MPa.

Atlikta lūžių analizė rodo, kad statinio ir ciklinio irimo procesui didelę įtaką turi nevienalytiškumo dariniai ir defektų (tuštumų) sankaupos, kurios iškraipo plyšio frontą ir galutinio suirimo zoną. Pagal galutinio suirimo zonos formą apskaičiuotos ciklinio irimo tąsumo reikšmės K_c = 10-26 MPa $\sqrt{\mathrm{m}}$. Iš gautų duomenų galima spręsti, ar ketus tinka konstrukciniams elementams gaminti.

M.K. Leonavičius, E. Stupak, A. Krenevičius, A. Norkus

FATIGUE STRENGTH INVESTIGATION OF FOUR TYPE CAST IRONS SPECIMENS

S u m m a r y

In this paper data about four types cast irons chemical composition, microstructure, static mechanical properties, durability and cyclic fracture toughness is given. Ultimate stress obtained using cylindrical specimens of diameters 8-14 mm with circular notch are σ_u = 403-692 MPa. Endurance limit values of notched specimens are σ_0 = 85-96 MPa.

The performed analysis of breaks shows that heterogeneities and defects (voids) formation have an influence on static and cyclic fracture, because they change the crack front and shape of final fracture's zone. The values of cyclic fracture toughness obtained according to the shape of final fracture's zone are K_c = 10-26 MPa $\sqrt{\mathrm{m}}$. The obtained data allows deciding about the suitability of cast irons for structural elements production.

Keywords: austempered ductile cast iron, durability.

Received May 11, 2011
Accepted June 13, 2012